AD

TECHNICAL REPORT ARBRL-TR-02052

A MODEL FOR BOMBLET EJECTION FROM MISSILES

Raymond Sedney

April 1978

US ARMY ARMAMENT RESEARCH AND DEVELOPMENT COMMAND
BALLISTIC RESEARCH LABORATORY
ABERDEEN PROVING GROUND, MARYLAND

Destroy this report when it is no longer needed.
Do not return it to the originator.

Secondary distribution of this report by originating or sponsoring activity is prohibited.

Additional copies of this report may be obtained from the National Technical Information Service, U.S. Department of Commerce, Springfield, Virginia 22161.

The findings in this report are not to be construed as an official Department of the Army position, unless so designated by other authorized documents.

The use of trade names or manufacturers' names in this report does not constitute indorsement of any commercial product.

UNCLASSIFIED

SECURITY CLASSIFICATION OF THIS PAGE *(When Data Entered)*

REPORT DOCUMENTATION PAGE		READ INSTRUCTIONS BEFORE COMPLETING FORM
1. REPORT NUMBER TECHNICAL REPORT ARBRL-TR-02052	2. GOVT ACCESSION NO.	3. RECIPIENT'S CATALOG NUMBER
4. TITLE *(and Subtitle)* A Model for Bomblet Ejection from Missiles		5. TYPE OF REPORT & PERIOD COVERED Final 6. PERFORMING ORG. REPORT NUMBER
7. AUTHOR*(s)* Raymond Sedney		8. CONTRACT OR GRANT NUMBER*(s)* RDT&E 1L161102AH43
9. PERFORMING ORGANIZATION NAME AND ADDRESS US Army Ballistic Research Laboratory (ATTN: DRDAR-BLL) Aberdeen Proving Ground, MD 21005		10. PROGRAM ELEMENT, PROJECT, TASK AREA & WORK UNIT NUMBERS
11. CONTROLLING OFFICE NAME AND ADDRESS US Army Armament Research & Development Command US Army Ballistic Research Laboratory (ATTN: DRDAR-BL) Aberdeen Proving Ground, MD 21005		12. REPORT DATE APRIL 1978 13. NUMBER OF PAGES 38
14. MONITORING AGENCY NAME & ADDRESS*(if different from Controlling Office)*		15. SECURITY CLASS. *(of this report)* Unclassified 15a. DECLASSIFICATION/DOWNGRADING SCHEDULE

16. DISTRIBUTION STATEMENT *(of this Report)*

Approved for public release; distribution unlimited.

17. DISTRIBUTION STATEMENT *(of the abstract entered in Block 20, if different from Report)*

18. SUPPLEMENTARY NOTES

19. KEY WORDS *(Continue on reverse side if necessary and identify by block number)*

Bomblet Ejection
Lance M251 Warhead
Centrifugal Force
Aerodynamic Force
Shear Layer

20. ABSTRACT *(Continue on reverse side if necessary and identify by block number)*

Ejection of bomblets from a missile which does not have an active ejector mechanism is studied. A model is developed for this process which yields a measure of ejection time, bomblet position at early times and trajectories. The model involves centrifugal (roll rate effect) and aerodynamic forces. A gross knowledge of the flow field is necessary and an estimate for forces on a bomblet while it is penetrating a shear layer is crucial. It is shown that a bomblet may be trapped in a separated flow pocket. Results from the model are consistent with some observations and have been useful in design and performance studies.

DD FORM 1 JAN 73 1473 EDITION OF 1 NOV 65 IS OBSOLETE

UNCLASSIFIED

SECURITY CLASSIFICATION OF THIS PAGE *(When Data Entered)*

TABLE OF CONTENTS

LIST OF ILLUSTRATIONS

LIST OF ILLUSTRATIONS (continued)

I. INTRODUCTION

Some missiles have warheads which carry a large number of bomblets as payload. These are deployed at a predetermined altitude and disperse over a wide area. The bomblets are designed to have self-induced spin which generates a Magnus-type lift; they are often called Magnus rotors. The spin also arms the fuze so that the bomblet is prepared to explode on impact. A variety of factors could interfere with the arming process. Among these is the process by which the bomblets are separated from the warhead and propelled into the free stream where they acquire their full spin. This process, called bomblet ejection, establishes the initial conditions for the subsequent flight.

The specific missile and warhead considered in analyzing ejection is the Lance with its M251 warhead. It carries about 800 bomblets which are essentially spheres (typically, diameter = 0.0572m) with ridges to impart spin. They are deployed at low supersonic or high subsonic missile speeds after line charges cut the missile skin into two panels. In older designs an active ejection system was used; e.g., "slings," activated by the line charges, propelled the bomblets away from the missile. In more recent designs an active ejector is not employed but the bomblets are usually ejected successfully. However, the governing physical process was not understood.

The purpose of this paper is to construct a model of the bomblet ejection process. A model of the process is constructed, rather than a physical description from first principles, because there are not enough data for the latter. It is specifically intended for small times; i.e., when the radial displacement of the bomblets is of the order of 10 d, where d is the bomblet diameter, or 1 missile diameter. The model has proven useful in the explanation of certain anomalies in the performance of the warhead.

Several possible mechanisms for ejection are examined: inertia forces, forces due to explosive line charges, pitching motion of the missile, and the roll rate of the missile. The last of these is found to be dominant. The important elements of the model are: the flow field after the panels have cleared the missile, the restraining force on the bomblet (which introduces the dynamic pressure) as it crosses a shear layer, and the roll rate of the missile. A straightforward calculation gives the ejection time as a function of roll rate, flow field, restraining force, and bomblet position. Despite a number of simplifications, it is felt that the essential features of the ejection process are modeled correctly.

An important conclusion is that the time for ejection is a sensitive function of roll rate for the range of rates used in practice. The time for ejection can become infinite for small roll rates, which implies that the bomblet is trapped in a pocket of separated flow. In reality this means ejection is delayed; the bomblets eventually clear

the missile, at times so large that the model no longer applies. As the roll rate approaches zero, the model predicts large ejection times for all bomblets. The basis for the model no longer exists since the effects which were negligible must become dominant if the roll rate goes to zero. An alternate model, not considered here, was developed which would give ejection even for zero roll rate; the results were quite different from those of the first model.

For system performance studies, a knowledge of bomblet ejection is useful in two ways. The model can give initial conditions for a detailed study of bomblet trajectories and spin. Rather than a deterministic approach, a statistical one can be used. The function of the model is then to provide correlation parameters; this will be discussed in a separate report. Its success provides some indirect, partial support for the validity of the model.

The only data available to evaluate the model are the time of appearance and the shape of the distribution of the bomblets, as determined from a few film records. It is difficult to obtain accurate readings from these records but they show that, typically, the bomblets first appear at 100 msec at which time they are about 0.61m from the missile. Results from the model are in general agreement with these observations. In one case the film records were clear enough to measure the shape of the distribution of bomblets. The calculated results are consistent with the measurement. Thus some basis for confidence in the model exists; no more than that can be said, at present.

II. THE BOMBLET EJECTION MODEL

There are three items to consider: (1) the forces acting on the bomblets other than the flow field forces, (2) the flow field, and (3) the force on a bomblet as it penetrates the shear layer.

The packing of the bomblets in the warhead must be discussed first. From the manner in which they are packed, the initial distribution of bomblets will vary with each warhead. Figure 1 shows an ideal distribution which gives the correct total number of bomblets; 3 rows are shown and the bomblets are numbered for later reference. In practice, the bomblets are not necessarily loaded in such a regular pattern and distribution would be somewhat different, but unknown. A choice of initial positions must be made, however, and the one shown in Figure 1 is convenient for calculations. The skin and nose are shown by dashed lines. At "event time" the skin panels and nose are blown off, leaving the configuration shown by the solid lines.

The missile flies at small angle of attack with a nominal roll rate of 5 rev/sec. Only supersonic flight at event time is considered. It takes about 10 msec for the panels to lift off and about 50 msec to complete the separation process. The fuze ring and pedestal may or may

not be lost at early times. After the panels and nose are removed a new flow field is established. From the correlations given in Reference 1, about 10 msec are required to establish the flow with the fuze ring in place and probably about the same without the fuze ring. A typical time of 10 msec will be used in the discussion of the forces that were examined vis a vis ejection. The parameters for a specific Lance flight will be used in making the following estimates.

A. Forces on the Bomblets, Excluding Flow Field Forces

Immediately after skin release the forces are:

(1) An inertia force which tends to move the bomblets to the front. This is caused by the sudden change in drag coefficient, ΔC_D, because the low drag nose is ejected. An adequate approximation is $\Delta C_D = 1.0$. The axial acceleration of the bomblets with respect to the missile is then $47.5 m/sec^2$. In 10 msec the bomblets are displaced axially 0.0023m. This effect will be neglected.

(2) Forces due to the line charge. Blast and detonation waves cause an impulsive force. The pressures are several MPa's but act only near the charge and last for about 10 μsec. This can be neglected. From the burning of detonation products there will be a residual pressure in the warhead volume, estimated to be 2.07MPa. This is relieved by an expansion wave propagating in from the moving panels; while the wave traverses a bomblet, an outward radial force acts on it. A rough model of this effect gives a maximum acceleration of $97.5 m/sec^2$ in a radial direction. In 10 msec the bomblet would move 0.0048m, if the acceleration were constant. But it lasts for about 1 msec. Therefore, this will be neglected.

(3) Pitching motion of the missile. When the nose and skin panels are removed, forces act on the missile that cause pitching motion. With respect to the missile some bomblets will accelerate in a direction normal to the missile axis. The information necessary to calculate the magnitude of this effect was not available. However, some estimates of it were made. In the first quarter-cycle, which lasts about 170 msec, bomblets on the windward side are displaced radially whereas those on the leeward side are not until the second quarter-cycle. Photographs of a number of flights, including subsonic and supersonic cases, show that the time for the bomblets to move about 1 missile diameter (about 0.61m for the Lance) ranges from 80 to 130 msec. Based on these times this mechanism does not seem plausible; nor does it from an estimate of displacements. If no other forces act, in 10 msec bomblet 1a, Figure 1, has a significant displacement, about 0.02m, but bomblets 28a or 7c

---

1. *M. S. Holden, "Establishment Time of Laminar Separated Flows," AIAA Journal, Vol. 9, No. 11, November 1971, pp. 2296-2298.*

would be displaced 0.002m, which is negligible. This implies that the aggregate of bomblets tips during ejection; there is no evidence for this. Although it has not been established that this mechanism can be neglected, it is much less plausible than the roll rate effect and, therefore, will not be considered further.

(4) Release of centrifugal constraint. The nominal roll rate is 5 rev/sec. When the skin is removed the bomblets will move tangentially, in a straight line at constant velocity if there are no other forces acting on the bomblet; see Figure 2a. For the inner row, a in Figure 1, with the diameter of the central tube 0.178m, the initial acceleration is 116m/sec^2 (11.8 g), the initial velocity is 3.69m/sec and in 10 msec a bomblet would be displaced radially 0.0056m. The same quantities for the outer row, c, are: 229m/sec^2 (23.3 g), 7.28m/sec, and 0.011m. For the case of no forces the radial motion is obtained from a simple calculation. The distance, r(t), from the missile axis to the bomblet center, at time t, is given by

$$r = a/\cos\ (\tan^{-1}\ 2\pi\Omega t) \tag{1}$$

where a = r(0) and Ω is the roll rate in rev/sec. Actually, there are forces, described in Section B below, that may even prevent the bomblet from being ejected at early times. These forces are an important part of the model, but if they are neglected for the moment, (1) gives, for Ω = 5 rev/sec, radial positions at t = 100 msec of 0.396m, 0.579m, and 0.762m for rows a, b and c respectively. These radial distances are in the neighborhood of those observed. Of course the bomblet distribution will not be correct because the other forces have been neglected, but even this overly simplified approach gives reasonable results. Release of the centrifugal constraint is the most plausible mechanism for bomblet ejection; it will now be incorporated into a model.

The spin of the bomblets and the ridges which cause it are ignored; they are treated as spheres with diameter d = 0.0572m. Only the motion of the center of mass of the bomblets will be described. The equations of motion are written in a cylindrical polar coordinate system fixed with respect to the missile. Since the missile decelerates this is not an inertial system. However, the axial deceleration is 1/14 that of a bomblet (or W/C_DA is 14 times greater) and will be neglected. For an inertial system, with x the axial coordinate along the center-line of the missile and r and ϕ polar coordinates in the plane x = constant, the equations of motion are

$$m\ (\ddot{r} - r\dot{\phi}^2) = F_r \tag{2}$$

$$mr^{-1}\ d(r^2\dot{\phi})/dt = F_\phi = 0 \tag{3}$$

$$m\ddot{x} = F_x \tag{4}$$

with initial conditions, at t = 0, when the flow is first established,

$$r = a \qquad \dot{r} = 0$$

$$\phi = 0 \qquad \dot{\phi} = a\omega$$

$$x = x_0 \qquad \dot{x} = 0 \quad .$$

Here m is the mass, 0.419kg, of the bomblet, x_0 and a are the initial axial and radial coordinates of the bomblet, ω is the roll rate in rad/sec, and the applied forces are F_r, F_ϕ, F_x. Assuming axial symmetry, there is no force in the ϕ direction and (3) can be integrated, giving

$$r^2\dot{\phi} = C_1 = a^2\omega \quad .$$

This equation is not integrated since the circumferential motion is not needed in the model. It is used to simplify (2). Thus the equations to be integrated are

$$\ddot{r} = C_1{}^2/r^3 + F_r/m \tag{5}$$

$$\ddot{x} = F_x/m \tag{6}$$

The term $C_1{}^2/r^3$ is the apparent centrifugal force which accelerates the bomblet even if there is no force; i.e., if $F_r = 0$. In that case (1) can be derived from (5); but this is the hard way to do it. If F_r and F_x are functions of r only the equations can be integrated by quadrature after using the substitutions $2\ddot{r} = d\dot{r}^2/dr$ and $\ddot{x} = \dot{r}d\dot{x}/dr$. In general, F_r and F_x are functions of both r and x so that a numerical integration is required.

B. The Flow Field

Although some parts of the flow field will certainly be unsteady we shall assume steady flow here. (There are some analogies with flow over a spiked-nose projectile which are useful in thinking about the flow field.) For the kind of bomblet distribution shown in Figure 1, the steady flow near the bomblets would have regions of attached and separated flow. Some schlieren pictures of the flow over a configuration similar to that of Figure 1 were available, Reference 2, and were used

---

2. *Private communication from Mr. A. Loeb.*

as a guide for approximating the flow field. The shear layer indicated in Figure 1 is drawn with the help of those pictures. The shear layer angle with respect to the x-axis, θ_s, varies between 0 and 20°. Actually, slightly negative values are possible and the pictures of Reference 2 can be interpreted to give $\theta_s = 25°$. At t = 0 most of the bomblets will be encased in the shear layer but the flow will attach on some of them; these will be subject to an additional force not considered in the next paragraph. Calculations have been made for a range of values of θ_s and for a bomblet on which the flow attaches. The shear layer is important because, until they penetrate it, the bomblets are shielded by it from the flow outside the shear layer which has high dynamic pressure, q. This external flow could be obtained from a calculation of the inviscid flow over the fuze ring and shear layer. Such sophistication is unwarranted; the flow variables immediately outside the shear layer were obtained from the flow over a flat-faced cylinder. Inside the shear layer, q and the aerodynamic forces are small. In Figure 2b two typical bomblets, which have moved from their original position, are shown. The only significant force acting on them is the centrifugal force until they reach the shear layer. The question then is: can a bomblet penetrate the shear layer?

C. A Model for Penetration of the Shear Layer by a Bomblet

The complicated interaction between a bomblet and the shear layer flow must be modelled in a simple way that retains the essence of the process. Specifically, an approximation to the forces on the bomblet is needed. Three assumptions are made for this purpose. First, the shear layer is replaced by a vortex sheet; i.e., an inviscid shear layer. Second, the shear layer remains fixed while a bomblet penetrates it. These are illustrated in Figure 2c; the small velocity inside the shear layer is taken to be zero. Let the components of the force on the bomblet, parallel and perpendicular to the shear layer, be F_n and F_s; the latter is called the restraining force. In principle, we could calculate the force on the bomblet as it passes through the vortex sheet, treating the flow as inviscid and quasi-steady. But the flow over a segment of a bomblet, position 2 in Figure 2c, is three-dimensional and such an elaborate calculation is unjustified and unacceptable for our purpose. There is one position of the bomblet where the calculation becomes simple, viz., that for which the bomblet center is on the vortex sheet, position 3 in Figure 2c. Then we have flow over a hemisphere. For this position we denote F_s and F_n by F_{sm} and F_{nh}, respectively. Experimentally determined pressure distributions over a sphere can be used to calculate F_{sm} and F_{nh}. The data of Reference 3 were used

---

3. *F. D. Bennett, W. C. Carter and V. E. Bergdolt, "Interferometric Analysis of Airflow about Projectiles in Free Flight," J. Applied Physics, Vol. 23, No. 4, April 1952, pp. 453-469.*

since they were was particularly well suited for this purpose. The free stream (or missile) Mach number is $M_\infty = 1.82$ for a typical flight for which results will be presented. Then $p = 0.5\ p_\infty$ and $M = 2.13$, where p and M are the pressure and Mach number outside the vortex sheet, at the position of bomblet 1a. Using the procedure just outlined we obtain

$$F_{sm} = 22.2N$$

$$F_{nh} = 200N \quad .$$

As a check on the calculation note that $2F_{nh} = 400N$ is within a few percent of the drag force obtained from the standard C_D for a smooth sphere. Because of the ridges on the bomblet F_{sm} and F_{nh} will be larger than the results for a smooth sphere; the magnitude of the increase depends on the orientation of the bomblet. The third assumption is that the forces are taken to be linear functions of s, the distance of the bomblet across the shear layer and that, in position 4, $F_s = 0$ and F_n = drag of a sphere. The resulting force distributions are illustrated in Figure 2d. Some obvious refinements to these force distributions could be made but, because of uncertainties in the physical processes we are trying to analyze and in other elements of the model, this is not justified in a first approximation. The forces that enter equations (5) and (6) are then

$$F_r(s) = -F_s(s) \cos \theta_s + F_n(s) \sin \theta_s \qquad (7)$$

$$F_x(s) = F_s(s) \sin \theta_s + F_n(s) \cos \theta_s \qquad (8)$$

where

$$s = (r - r_0) \cos \theta_s - (x - x_0) \sin \theta_s$$

and r_0 is the r coordinate of the center of the bomblet when it is tangent to the shear layer, as in position 1 in Figure 2c. Each F in (7) and (8) is a linear function of s, or constant; they are zero for $s \leq 0$. The bomblet accelerates in the r direction under the influence of centrifugal force but its axial coordinate is fixed at $x = x_0$ until it becomes tangent to the shear layer. It then feels the effect of both F_r and F_x. If its radial momentum plus the centrifugal effect are large enough to overcome F_r, the bomblet penetrates the shear layer and is ejected.

The motion is easily illustrated for the special case $\theta_s = 0$ because (5) can be integrated once. Consider row a so that $r_0 = a$ and $s = r - a$. Then from Figure 2d, where $s = d/2$ at position 3, and (7),

$$F_r = - F_s = - 2F_{sm} (r-a)/d \qquad \text{for } a \leqslant r \leqslant a + (d/2) \qquad (9)$$

$$= - 2F_{sm} [d - (r-a)]/d \qquad \text{for } a + (d/2) \leqslant r \leqslant a + d, \qquad (10)$$

Using these and $2\ddot{r} = d\dot{r}^2/dr$ in (5) yields

$$\dot{r}^2 = a^4\omega^2 (a^{-2}-r^{-2}) - 2F_{sm} (r-a)^2/md \qquad (11)$$

and

$$\dot{r}^2 = a^4\omega^2 (a^{-2}-r^{-2}) + [d^2 - 4d(r-a) + (r-a)^2] F_{sm}/md \qquad (12)$$

for the two ranges of r given in (9) and (10) respectively. For the values of the parameters a = 0.117m, d = 0.0572m, m = 0.419kg and using F_{sm} = 35.6N, $\dot{r}$ vs r is plotted in Figure 3 for various $\Omega = \omega/2\pi$; t is a parameter along each curve with t = 0 at r = a. The bomblet penetrates the shear layer for Ω = 4.5 rev/sec, curve A, but does not for any of the other curves. As Ω decreases the bomblet continues to escape, but the time to do so increases, until a limiting value, Ω_ℓ, is reached; here Ω_ℓ = 4.129 rev/sec. For this curve B, (12) has a double root and the time to reach that value of r is infinite. For curves C, D, and E the bomblet would oscilate between r = a and the other for which $\dot{r} = 0$, according to this idealized model.

In summary, after the bomblets have been exposed and the flow established, the forces are defined by a knowledge of the shear layer, the inviscid flow outside the shear layer, and the forces acting on a hemisphere at the local flow conditions. The magnitude of these forces depends on the dynamic pressure. Since it is expected that this model will yield only estimates or be used for comparative purposes, a precise knowledge of the flow field is not necessary. For example, if the missile is at angle of attack, the angle and position of the shear layer can be estimated from wind tunnel or ballistic range shadowgraphs of configurations that approximate the warhead plus bomblets. In any case, to obtain useful results, the parameters will have to be varied from their initial estimates because of the number of simplifying assumptions incorporated in the model.

III. RESULTS

The model was used to calculate some results pertinent to ejection for a typical supersonic flight of the Lance. The velocity at event time is taken as 609.6m/sec ($M_\infty = 1.82$) and zero angle of attack is assumed. The input quantities are x_o, a, θ_s, F_{sm}, F_{nh}, and the roll rate in rev/sec, Ω. In Figure 1 θ_s varies between 0° and 20°. To simplify matters the results are presented for a constant θ_s for all bomblets or for one specific bomblet. It is more tedious to do the calculations using the θ_s corresponding to each bomblet. Of course, as the bomblets penetrate the shear layer, θ_s changes. This interaction and that of one bomblet with another are neglected; the motion of each bomblet is treated without regard to another. Note that, for a constant $\theta_s = 5°$, the shear layer would be a straight line joining the fuze ring and the rear wall of the cargo compartment.

The model should answer the questions: will the bomblets penetrate the shear layer and if so how long will it take? The ejection time, t_e, is defined as the time for a bomblet to be displaced radially one diameter, across the shear layer; it is the time between positions 1 and 4 in Figure 2c and is also indicated in Figure 4.

For bomblet 1a, see Figure 1, t_e vs. Ω, for various θ_s, is presented in Figure 4. For smaller Ω, t_e is a sensitive function of θ_s. In fact each curve has an asymptote for some Ω; i.e., $t_e \to \infty$, which means the bomblet never penetrates the shear layer; it is trapped under the shear layer. Figure 5 applies to all bomblets in row a and shows t_e vs Ω for $\theta_s = 0$ for a range of F_{sm} above and below the value of 22.2N derived in the last section for a smooth sphere. $F_{sm} = 0$ implies $F_r = 0$, which was discussed in the last section; the motion is determined by (1) which also gives the equation of the dashed curve in Figure 4:

$$2\pi\Omega t_e = \tan\left[\cos^{-1}\left(\frac{a}{a+d}\right)\right] \quad .$$

This has an asymptote at $\Omega = 0$. For each F_{sm} there is an asymptote at $\Omega = \Omega_\ell$; the relationship between Ω_ℓ and F_{sm} is shown in Figure 6 for $\theta_s = 0$. For comparison, the values for two other θ_s are given: for $\theta_s = 10°$, $\Omega_\ell = 3.8$ rev/sec and $F_{sm} = 23.8$N; for $\theta_s = 30°$, $\Omega_\ell = 4.3$ rev/sec and $F_{sm} = 22.2$N. The asymptote is easily explained physically. If the radial momentum plus the centrifugal effect are large enough to overcome

the radial component of force, the bomblet is ejected; i.e., t_e is finite. When these just balance $t_e \to \infty$. Thus, decreasing Ω, increasing F_{sm}, or increasing θ_s will force the bomblet back into the shear layer and it will not be ejected; this behavior is shown in computed trajectories. The correct interpretation of this result is that the ejection time becomes large, by which time the angle of attack of the missile is so large that the model can no longer be used without modification.

Trapping of a bomblet and the existence of Ω_ℓ was explained earlier using Figure 5 for the special case $\theta_s = 0$. In principle Ω_ℓ can be found by determining the Ω for which (12) has double roots. Since the roots of a quartic must be found, a convenient, general expression for Ω_ℓ (F_{sm}) can be given; however, it is obvious from (12) that $\Omega_\ell \propto F_{sm}^{\frac{1}{2}}$. A convenient expression for $\Omega_o(F_{sm})$ can be found, where Ω_o is determined from $\dot{r} = 0$ at $r = a+d$; see curve C for which the dashed portion has no physical meaning. The result is

$$\Omega_o^2 = (a+d)^2 F_{sm}/4\pi^2 a^2 m (2a+d)$$

Since Ω_o is within a few percent of Ω_ℓ, this expression is adequate considering the approximate nature of the model.

The sensitivity of t_e to Ω, for a given F_{sm}, is not the same for all bomblets, even for a constant θ_s. Figure 7 shows t_e vs Ω for rows a, b, and c of Figure 1. Because $\theta_s = 0$, t_e is the same for all bomblets in a row. The results for row a (already given in Figure 5) show that t_e for these bomblets is more sensitive to decreasing Ω than it is for rows b and c. This is because the centrifugal force acting on them, through the factor C_1 in (5), is greater.

The definition of t_e does not account for the time it takes for a bomblet to move up to the shear layer, t_i, which can be obtained from (1). The total time for a bomblet to get across the shear layer is $t_i + t_e$. This is shown in Figure 8 for $\theta_s = 5°$, $F_{sm} = 22.2N$ and two roll rates, 3.8 and 5.0 rev/sec. For the 3.8 case the two times for bomblet 28a are $t_i = 79.7$ msec and $t_e = 26$ msec; for bomblet 1a, $t_i = 0$ and $t_e = 66.6$ msec. t_e is smaller for 28a because of its greater momentum when it reaches the shear layer. The non-monotonic behavior for row a with $\Omega = 3.8$ rev/sec is an indication that the first few bomblets are close to the asymptote.

A knowledge of t_e and t_i are useful in design and performance studies and the existence of the asymptote is an important result from the model. Considering the various θ_s appropriate to the bomblets we can conclude that only a fraction of the bomblets would be trapped for certain Ω and F_{sm}.

Trajectories for bomblets 1a, 1b, 1c, and 28a are shown in Figure 9 with Ω = 3.8 rev/sec and $\theta_s = 5°$; the velocities, relative to the missile, at t = 120 msec are also listed. Note the different scales in the axial and radial directions. After ejection the point mass trajectories are computed with $F_s = 0$ and $F_n = 2F_{nh}$ which means that the direction of the force is fixed at an angle θ_s with respect to the missile axis. The lift on a bomblet is neglected. The three dots on each trajectory locate t = 80, 100, and 120 msec. There are some obvious uses for the trajectories; e.g., determining if a control surface is struck by a bomblet.

The distribution of all bomblets at t = 100 msec is shown in Figure 10, for Ω = 3.8 rev/sec and F_{sm} = 22.2N. The shear layer angle was taken to be constant; $\theta_s = 10°$ was chosen to give the best agreement with a test result discussed below. The positions of rows a, b, and c are shown by curves; the first and last bomblets in each row are indicated by a dot and are numbered; the other dots show the positions of bomblets whose number is a multiple of 5. The spherical bomblet appears to be elliptical because of the different x and r scales. The distribution shows that some bomblets would have collided, an effect which is neglected. For a test in which Ω = 3.8 rev/sec, the bomblets could be discerned in a photograph, from the ground, taken at t = 100 msec; the bomblets appear as a dark cloud near the missile. The leading edge of this cloud is shown in Figure 10 as a dashed straight line connecting the two end points which have error bars attached. The quality of the photograph did not permit a more accurate measurement. The perspective of the photograph does not allow the distribution of bomblets to be determined but the leading edge can be compared with the front of the calculated distribution. The agreement between these is close enough to give confidence in the model.

The effect on the distribution of changing Ω is shown in Figure 11. As expected, the radial displacement of the bomblets is greater for the larger Ω; the axial displacement is also increased. For $\Omega < 3.8$ rev/sec some of the bomblets would not appear in the distribution since they would have been trapped by the shear layer.

IV. CONCLUSIONS

The problem of bomblet ejection from missiles which do not have an active ejection system has been studied. A model was formulated for the ejection process, the crucial elements of which are the centrifugal effect due to the spin of the missile and the interaction of the bomblets with the shear layer. An ejection time is defined which can be used as a measure of the effect of various parameters on the ejection process. For a given shear layer angle and restraining force, this time becomes infinite as the roll rate decreases. Taken literally, this implies that a bomblet will be trapped under the shear layer. Realistically it means that the time for ejection is large, at which time the conditions for the model's validity are not met. Such delayed ejection can affect the performance of the system. Bomblet trajectories and distributions have also been presented. In one case, the calculated distribution is compared with the shape of the distribution determined in a test. The agreement is favorable enough to lend credence to the model.

ACKNOWLEDGMENTS

In various aspects of this work, I received help from Mr. B. Bertram, Mr. W. Chase, Mr. N. Gerber, Mr. G. Kahl, Dr. C. Kitchens, and Prof. M. Morkovin. I especially thank Ms. J. Bartos who did all of the calculations and aided in preparing this report.

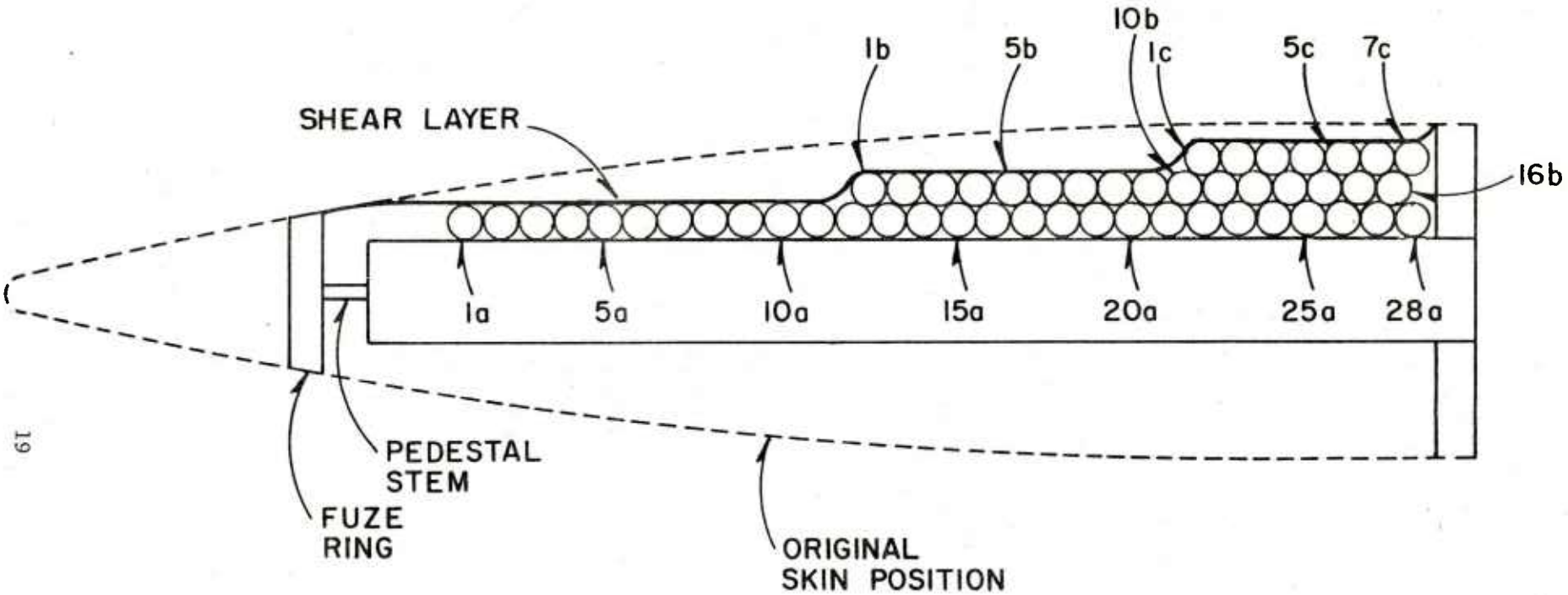

Figure 1. Sketch of a missile warhead containing an idealized packing of bomblets in three rows: a, b, and c. The shear layer is formed after the dashed line configuration is removed.

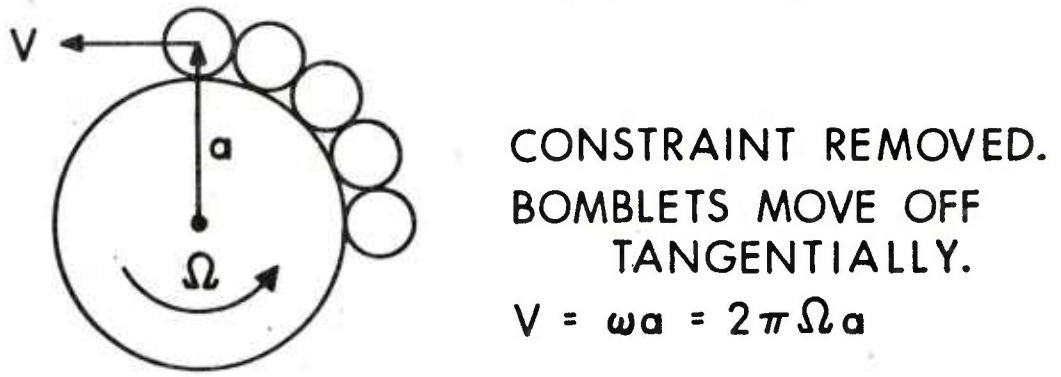

Figure 2. The Elements of the Bomblet Ejection Model.

(a) A cross-sectional view of some bomblets on the central tube, after release of the centrifugal constraint.

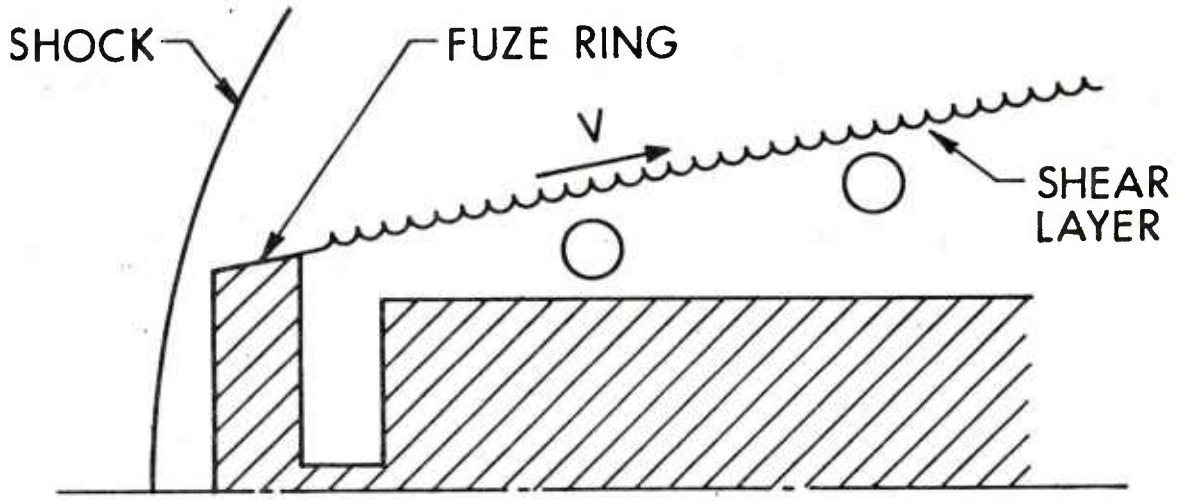

Figure 2. Continued

(b) Two typical bomblets moving toward the shear layer, with only centrifugal force acting.

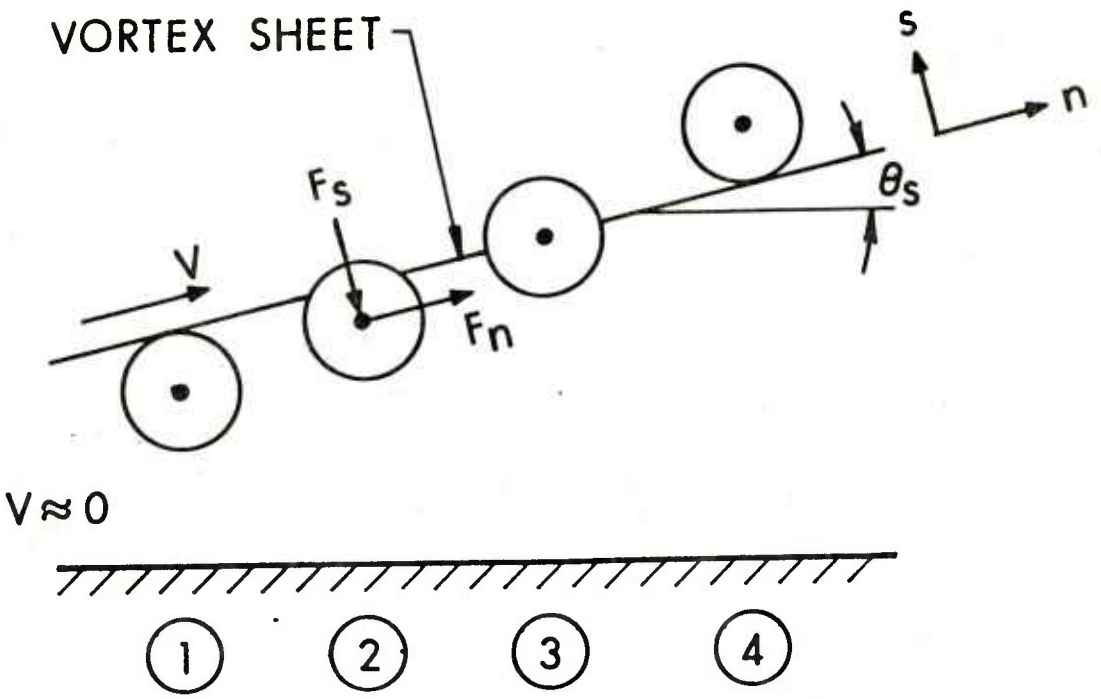

Figure 2. Continued
(c) Bomblet penetration of the vortex sheet.

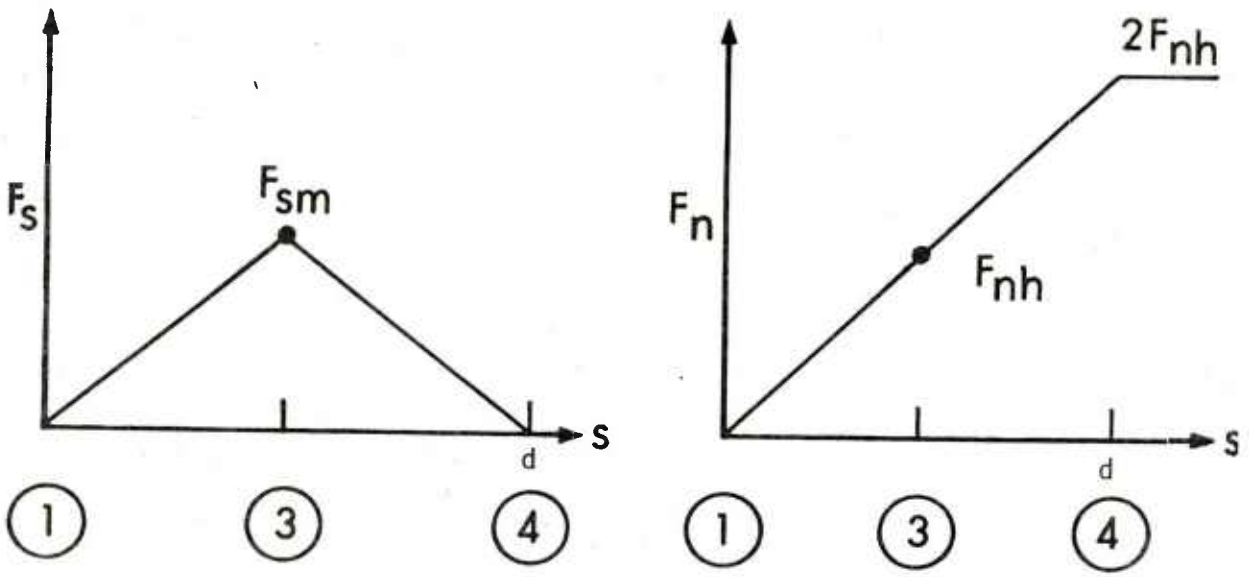

Figure 2. Concluded
(d) Assumed force distribution.

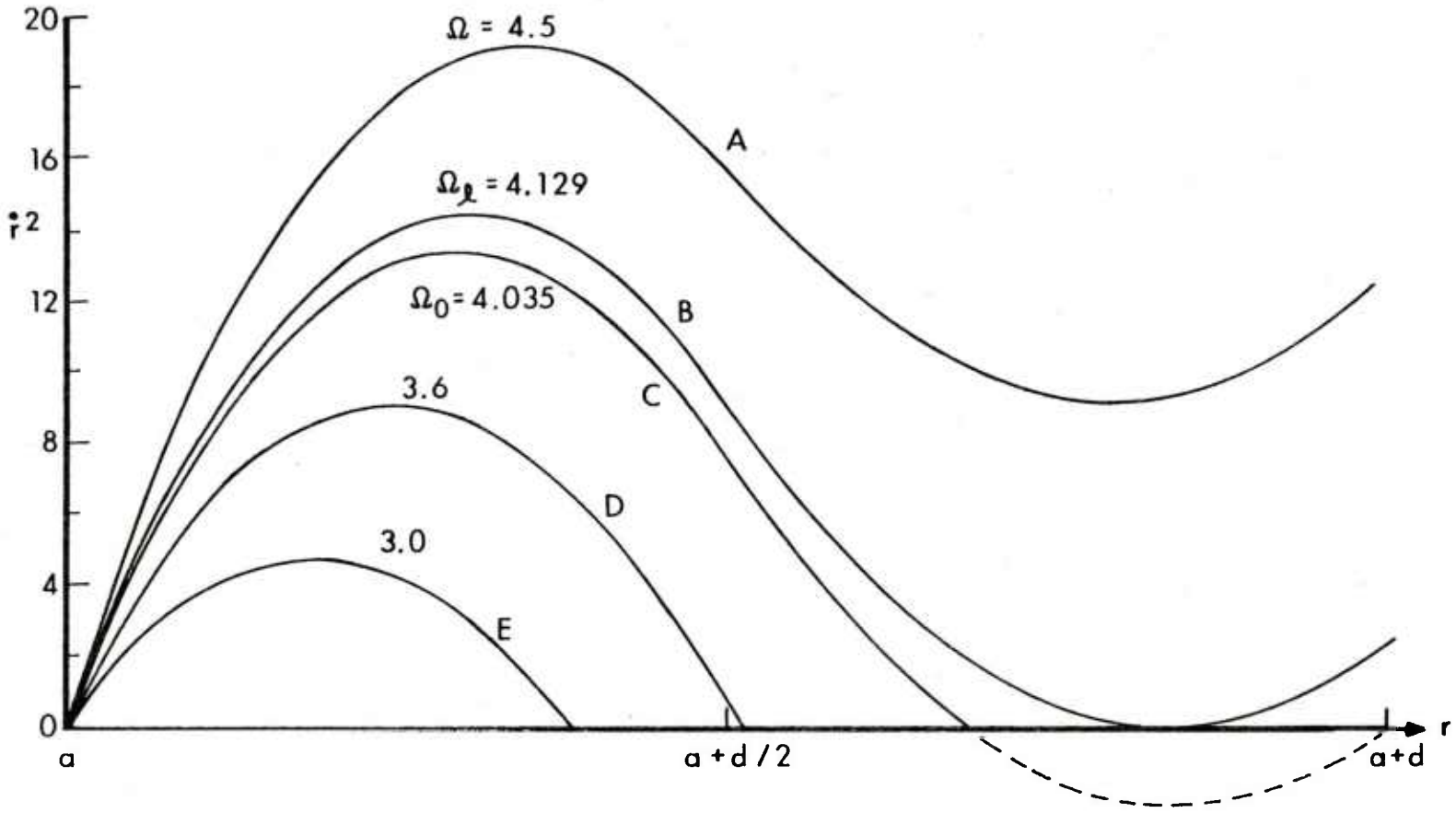

Figure 3. Phase plane diagram, $\dot{r}^2$ vs r, of the motion of a bomblet in row a for $\theta_s = 0$, F_{sm} = 35.6N (8lbf), m = 0.419kg (.0287 slugs), a = 0.117m, d = 0.0572m and Ω (rev/sec) as a parameter.

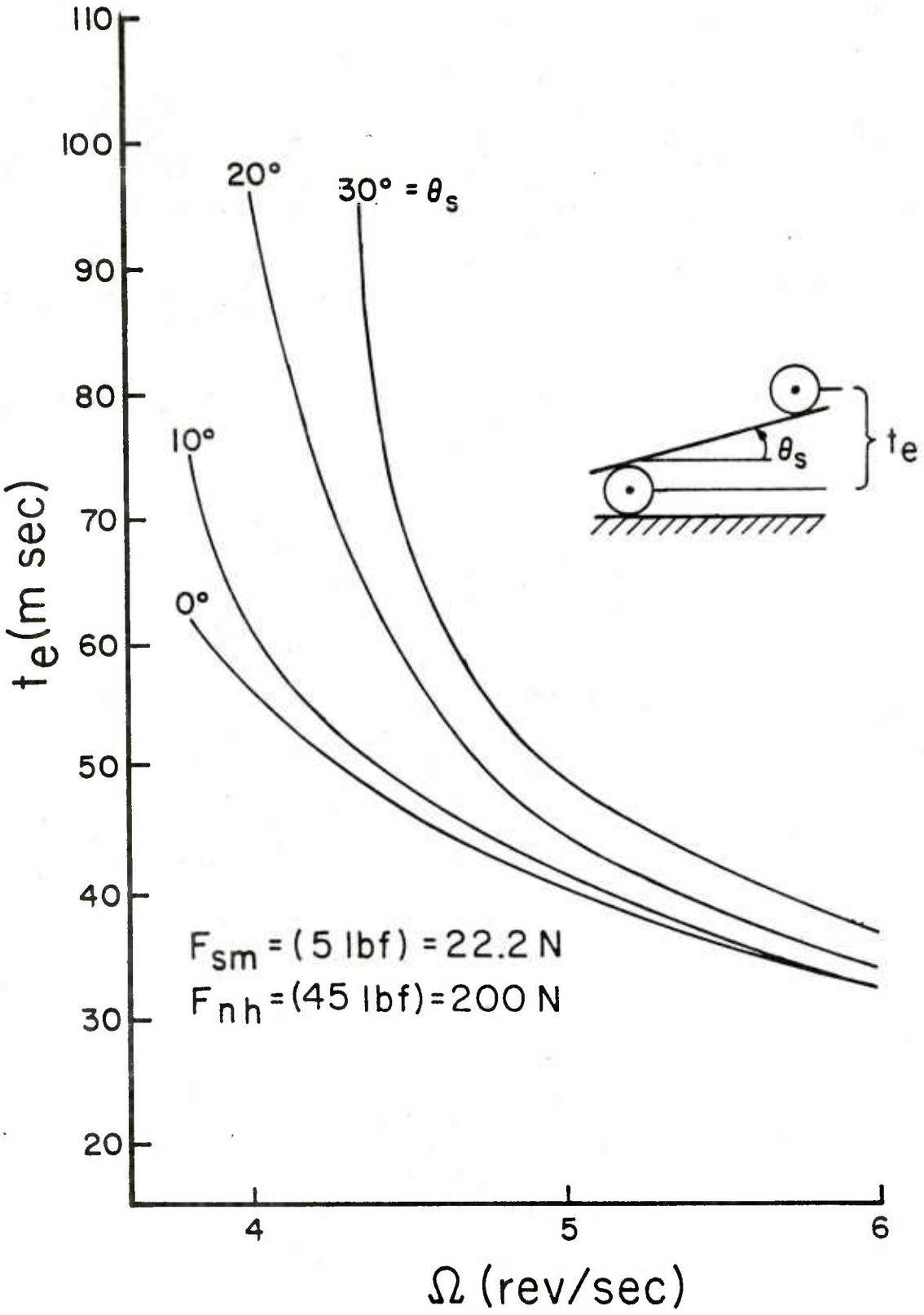

Figure 4. For bomblet 1a, ejection time vs. roll rate, with shear layer angle as the parameter.

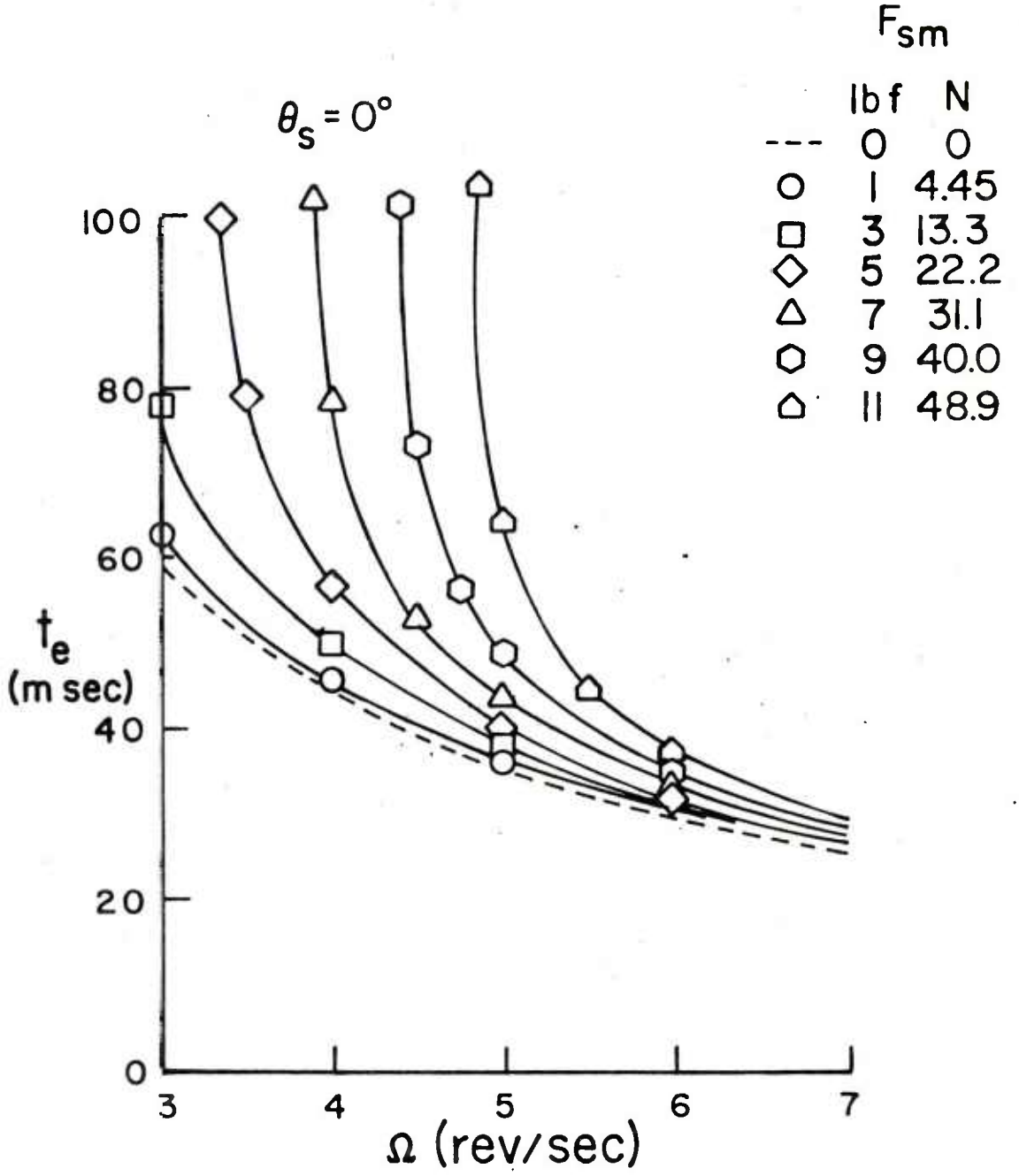

Figure 5. For all bomblets in row a, ejection time vs. roll rate, with restraining force as parameter.

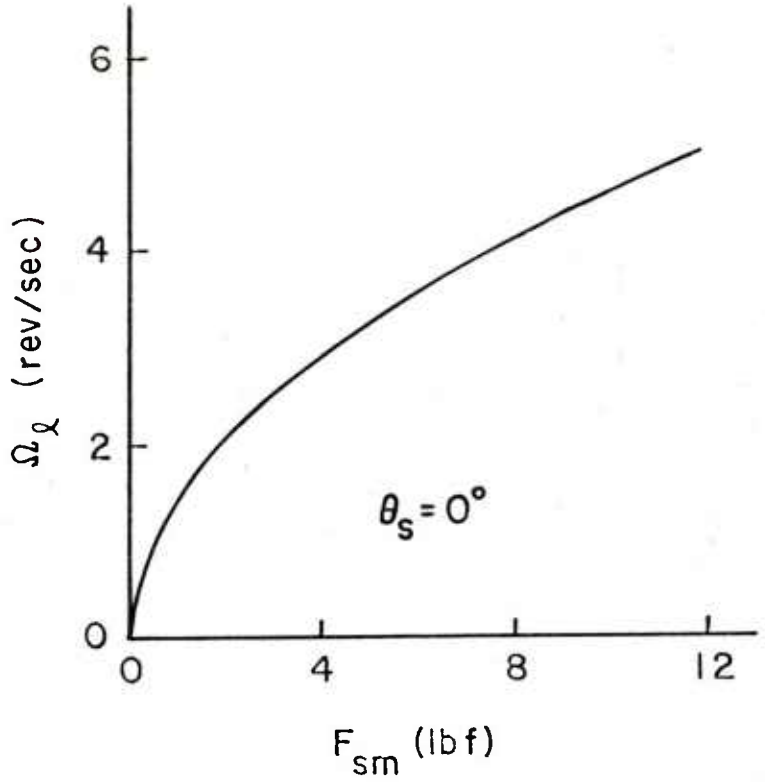

Figure 6. The limiting roll rate at which $t_e \to \infty$, for all bomblets in row a, vs. the restraining force.

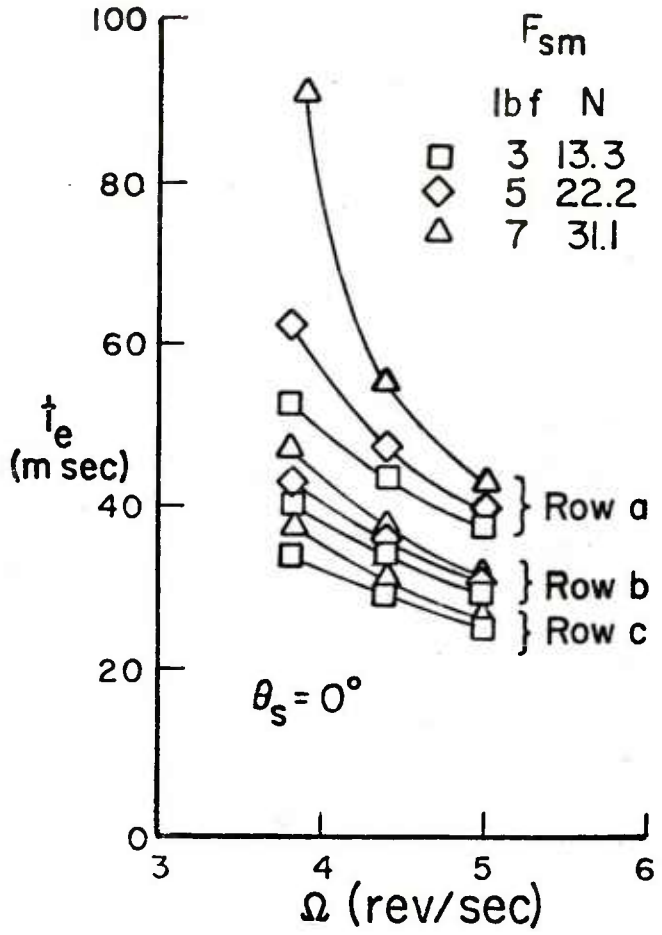

Figure 7. For all bomblets in rows a, b, and c, ejection time vs. roll rate, with restraining force as parameter.

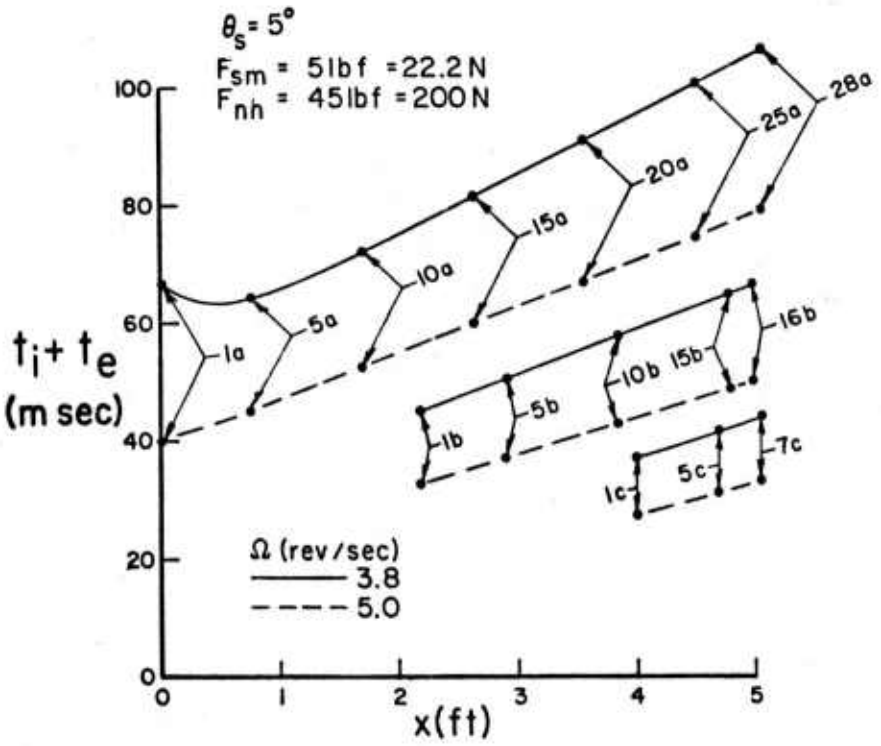

Figure 8. The total time for each bomblet to get across the shear layer vs. its axial coordinate at t = 0, for two roll rates.

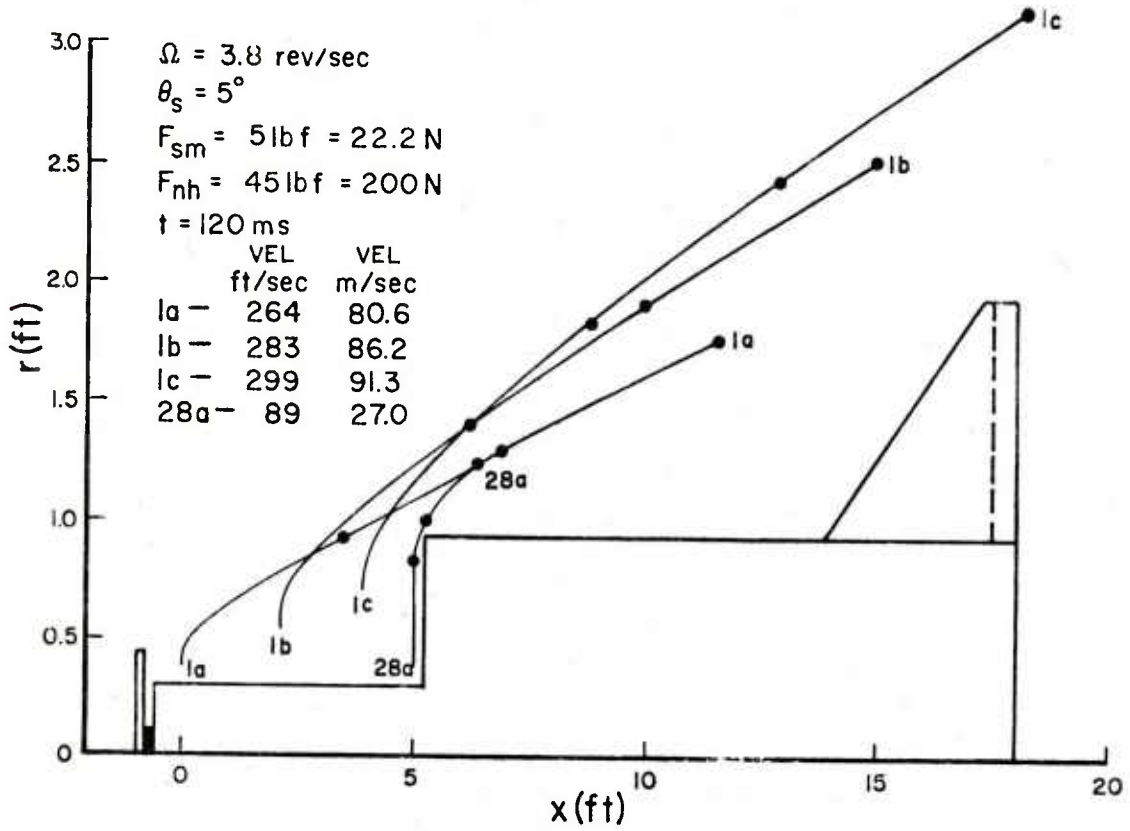

Figure 9. Trajectories for bomblets 1a, 1b, 1c, and 28a and their velocity at t = 120 msec. The three dots on each trajectory are at t = 80, 100, and 120 msec.

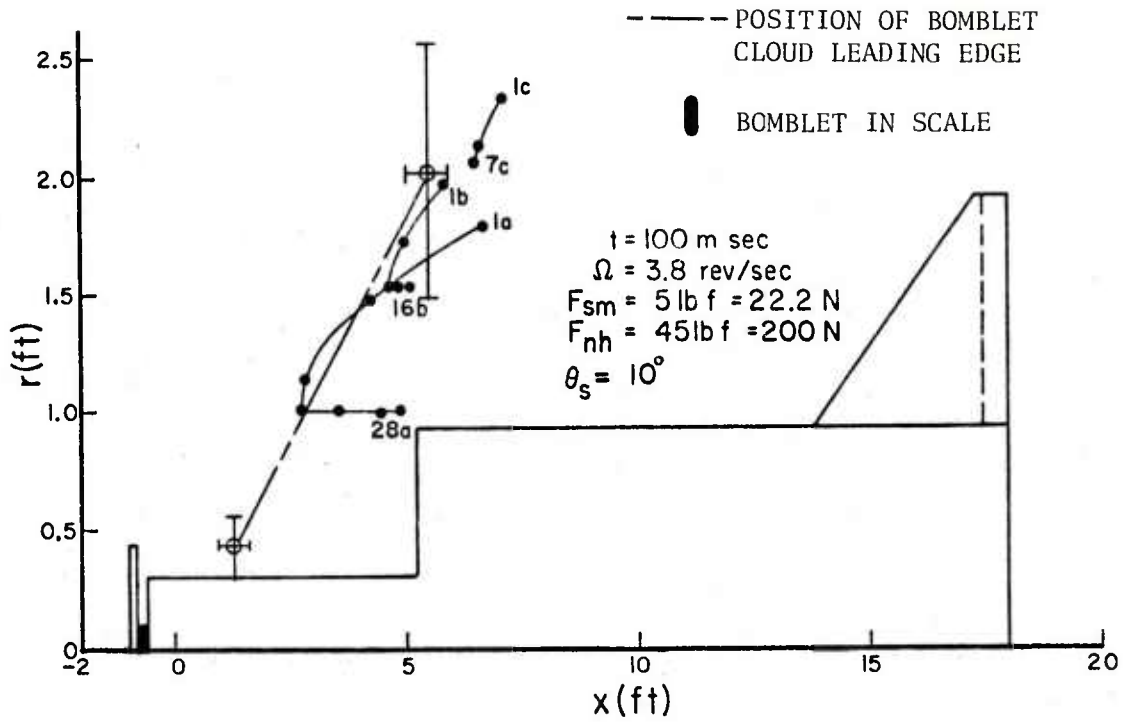

Figure 10. The solid curves through the dots give the distribution at t = 100 msec of the bomblets initially in rows a, b, and c. The significance of the dots is given in the text. The dashed line is obtained from a test result.

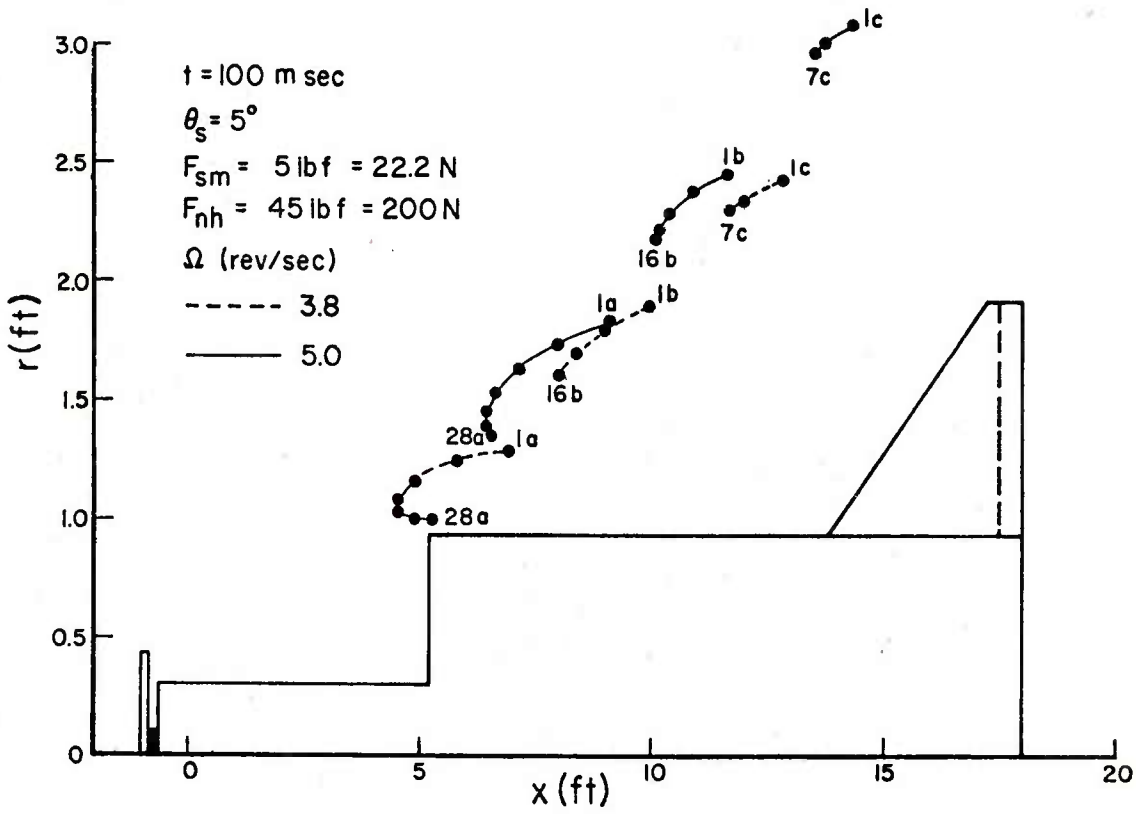

Figure 11. The distribution at t = 100 msec of the bomblets initially in rows a, b, and c for two roll rates. The significance of the dots is the same as in Fig. 9.

LIST OF SYMBOLS

a	initial radial coordinate of bomblet center of mass (m)
d	diameter of bomblet (m)
m	mass of bomblet (kg)
p	pressure at the vortex sheet (MPa)
p_∞	free stream pressure (MPa)
q	dynamic pressure (MPa) = $\frac{1}{2} \rho_\infty V_\infty^2$
r_0	r-coordinate of the center of mass of the bomblet when it is tangent to the shear layer (m)
s,n	coordinates perpendicular and parallel to the shear layer (m)
t	time (sec, msec)
t_e	ejection time (sec, msec)
t_i	time it takes the bomblet to move up to the shear layer (sec, msec)
x, r, ϕ	cylindrical polar coordinates fixed with respect to the missile (m)
x_0	initial axial coordinate of the bomblet center of mass (m)
A	cross-sectional area of bomblet or missile (m^2)
C_D	drag coefficient
C_1	constant in equation preceding equation (5) (= $a^2\omega$)
F_s, F_n	forces perpendicular and parallel to shear layer (N)
F_{sm}, F_{nh}	F_s, F_n respectively at that position where the bomblet center is on the vortex sheet (N)
F_x, F_r, F_ϕ	components of applied force in cylindrical coordinates (N)

LIST OF SYMBOLS (continued)

M	Mach number outside vortex sheet
M_∞	free stream (or missile) Mach number
V	velocity external to the vortex sheet (m/sec)
V_∞	free stream velocity or missile velocity at event (m/sec)
W	weight of bomblet or missile (N)
ρ_∞	atmospheric density at event height (kg/m^3)
ω	roll rate (rad/s)
θ_s	shear layer angle with respect to the x-axis
Ω	roll rate (rev/sec)
Ω_ℓ	asymptotic value of roll rate (rev/sec)
$\cdot$	differentiation with respect to time (d/dt)

DISTRIBUTION LIST

No. of Copies	Organization
12	Commander Defense Documentation Center ATTN: DDC-TCA Cameron Station Alexandria, VA 22314
1	Commander US Army Materiel Development and Readiness Command ATTN: DRCDMA-ST 5001 Eisenhower Avenue Alexandria, VA 22333
1	Commander US Army Aviation Research and Development Command ATTN: DRSAV-E 12th and Spruce Streets St. Louis, MO 63166
3	Commander US Army Air Mobility Research and Development Laboratory ATTN: SAVDL-D W.J. McCroskey W.F. Ballhaus Mail Stop 202-1 Ames Research Center Moffett Field, CA 94035
1	Commander US Army Electronics Command ATTN: DRSEL-RD Fort Monmouth, NJ 07703
3	Commander US Army Missile Research and Development Command ATTN: DRDMI-RD DRDMI-R Mr. R. Deep Redstone Arsenal, AL 35809
1	Commander US Army Tank Automotive Research & Development Cmd ATTN: DRDTA-RWL Warren, MI 48090
2	Commander US Army Mobility Equipment Research & Development Cmd ATTN: Tech Docu Cen, Bldg. 315 DRSME-RZT Fort Belvoir, VA 22060
1	Commander US Army Armament Materiel Readiness Command ATTN: DRSAR-LEP-L, Tech Lib Rock Island, IL 61299
4	Commander US Army Armament Research and Development Command ATTN: DRDAR-LCA-F Mr. A. Loeb Mr. H. Hudgins DRDAR-LCU-D-R Mr. T. Stevens Dover, NJ 07801
1	Commander US Army Harry Diamond Labs ATTN: DRXDO-TI 2800 Powder Mill Road Adelphi, MD 20783
1	Director US Army TRADOC Systems Analysis Activity ATTN: ATAA-SL, Tech Lib White Sands Missile Range NM 88002

DISTRIBUTION LIST

No. of Copies	Organization
1	Project Manager LANCE Missile System US Army Missile Materiel Readiness Command ATTN: DRCPM-LC Redstone Arsenal, AL 35809
2	Commander US Army Research Office ATTN: R. E. Singleton E. Saibel P. O. Box 12211 Research Triangle Park NC 27709
1	Commander US Army Waterways Experiment Station ATTN: R. H. Malter Vicksburg, MS 39180
1	AGARD-NATO ATTN: R. H. Korkegi APO New York 09777
3	Commander US Naval Air Systems Command ATTN: AIR-604 Washington, DC 20360
3	Commander US Naval Ordnance Systems Command ATTN: ORD-0632 ORD-035 ORD-5524 Washington, DC 20360
2	Commander David W. Taylor Naval Ship Research & Development Cmd ATTN: H. J. Lugt, Code 1802 S. de los Santos Head, High Speed Aerodynamics Division Bethesda, MD 20084
1	Commander Naval Surface Weapons Center ATTN: DX-21, Library Br. Dahlgren, VA 22448
5	Commander Naval Surface Weapons Center Applied Aerodynamics Division ATTN: K. R. Enkenhus R. Lee S. M. Hastings A. E. Winklemann W. C. Ragsdale Silver Spring, MD 20910
1	AFATL (DLDL, Dr. D.C. Daniel) Eglin AFB, FL 32542
2	AFFDL (W.L. Hankey; J.S.Shang) Wright-Patterson AFB, OH 45433
5	Director National Aeronautics and Space Administration ATTN: D. R. Chapman J. D. Murphy J. Rakich W. C. Rose B. Wick Ames Research Center Moffett Field, CA 94035
3	Director National Aeronautics and Space Administration ATTN: J. South J. R. Sterrett Technical Library Langley Station Hampton, VA 23365

DISTRIBUTION LIST

No. of Copies	Organization
1	Director National Aeronautics and Space Administration Lewis Research Center ATTN: MS 60-3, Tech Lib 21000 Brookpark Road Cleveland, OH 44135
1	Director National Aeronautics and Space Administration Marshall Space Flight Center ATTN: S&E-AERO-AE A. R. Felix, Chief Huntsville, AL 35812
2	Director Jet Propulsion Laboratory ATTN: J. Kendall Technical Library 4800 Oak Grove Drive Pasadena, CA 91103
3	ARO, Inc. ATTN: J. D. Whitfield R. K. Matthews J. C. Adams, Jr. Arnold AFB, TN 37389
3	Aerospace Corporation ATTN: T. D. Taylor H. Mirels R. L. Varwig Aerophysics Lab P. O. Box 92957 Los Angeles, CA 90009
1	Alpha Research, Inc. ATTN: J. E. Brunk 55 Hitchcock Way, Suite 103 Santa Barbara, CA 93105
1	AVCO Systems Division ATTN: B. Reeves 201 Lowell Street Wilmington, MA 01887
3	The Boeing Company Commercial Airplane Group ATTN: W. A. Bissell, Jr. Mail Stop 1W-82 P. E. Rubbert J. D. McLean Seattle, WA 98124
2	Calspan Corporation ATTN: A. Ritter M. S. Holden P. O. Box 235 Buffalo, NY 14221
1	Center for Interdisciplinary Programs ATTN: Victor Zakkay W. 177th St & Harlem River Bronx, NY 10453
1	General Dynamics ATTN: Research Lib 2246 P O Box 748 Fort Worth, TX 76101
1	General Electric Company, RESD ATTN: R. A.Larmour 3198 Chestnut Street Philadelphia, PA 19101
1	Grumann Aerospace Corporation ATTN: R. E. Melnik Research Department Bethpage, NY 11714
2	Lockheed-Georgia Company ATTN: B. H. Little, Jr. G. A. Pounds Dept 72074, Zone 403 86 South Cobb Drive Marietta, GA 30062
1	Lockheed Missiles & Space Co. ATTN: Tech Info Center 3251 Hanover Street Palo Alto, CA 94304

DISTRIBUTION LIST

No. of Copies	Organization
4	Martin-Marietta Laboratories ATTN: S. H. Maslen S. C. Traugott R. Goldman H. Obremski 1450 S. Rolling Road Baltimore, Maryland 21227
2	McDonnell-Douglas Astronautics Corporation ATTN: J. Xerikos H. Tang 5301 Bolsa Avenue Huntington Beach, CA 92647
1	McDonnell-Douglas Corporation Douglas Aircraft Company ATTN: T. Cebeci 3855 Lakewood Boulevard Long Beach, CA 90801
1	Northrup Corporation Aircraft Division ATTN: S. Powers 3901 West Broadway Hawthorne, CA 90250
2	Sandia Laboratories ATTN: F. G. Blottner Technical Library Albuquerque, NM 87115
1	Vought Corporation Michigan Division ATTN: Paul Meyer 38111 Van Dyke Avenue Warren, Michigan 48090
1	Vought Systems Division LTV Aerospace Corporation ATTN: J. M. Cooksey, 2-53700 Chief, Gas Dynamics Lab. P. O. Box 5907 Dallas, Texas 75222
3	California Institute of Technology ATTN: Technical Library H. W. Liepmann D. Coles Aeronautics Dept. Pasadena, CA 91109
2	Cornell University Graduate School of Aero Engr ATTN: Library F. K. Moore Ithaca, NY 14850
2	Illinois Institute of Technology ATTN: M. V. Morkovin H. M. Nagib 3300 South Federal Chicago, Illinois 60616
3	The Johns Hopkins University ATTN: S. H. Davis S. Corrsin L. S. G. Kovasznay Dept. of Mechanics & Materials Science Baltimore, MD 21218
1	Louisiana State University Department of Physics ATTN: R. G. Hussey Baton Rouge, LA 70803
2	Massachusetts Institute of Technology ATTN: E. Covert Technical Library 77 Massachusetts Avenue Cambridge, MA 02139

DISTRIBUTION LIST

No. of Copies	Organization
2	North Carolina State University Mechanical and Aerospace Engineering Department ATTN: F. F. DeJarnette J. C. Williams Raleigh, NC 27607
1	Notre Dame University ATTN: T. J. Mueller Dept. of Aero Engr South Bend, IN 46556
2	Ohio State University Department of Aeronautical and Astronautical Engineering ATTN: S. L. Petrie O. R. Burggraf Columbus, Ohio 43210
2	Polytechnic Institute of New York ATTN: G. Moretti S. G. Rubin Route 110 Farmingdale, NY 11735
4	Princeton University James Forrestal Research Center Gas Dynamics Laboratory ATTN: S. I. Cheng I. E. Vas S. M. Bogdonoff Technical Library Princeton, NJ 08540
1	Purdue University Thermal Science and Prop Center ATTN: D. E. Abbott W. Lafayette, IN 47907
1	Rensselaer Polytechnic Institute Department of Mathematical Sciences ATTN: R. C. DiPrima Troy, NY 12181
1	Rutgers University Department of Mechanical, Industrial and Aerospace Engineering ATTN: R. H. Page New Brunswick, NJ 08903
1	Southern Methodist University Department of Civil and Mechanical Engineering ATTN: R. L. Simpson Dallas, Texas 75275
1	Southwest Research Institute Applied Mechanics Reviews 8500 Culebra Road San Antonio, Texas 78228
1	University of California-Berkeley Department of Aerospace Engineering ATTN: M. Holt Berkeley, CA 94720
1	University of California-Davis ATTN: H. A. Dwyer Davis, CA 95616
2	University of California-San Diego Department of Aerospace Engineering and Mechanical Engineering Sciences ATTN: P. Libby Technical Library La Jolla, CA 92037

DISTRIBUTION LIST

No. of Copies	Organization
2	University of Cincinnati Dept of Aerospace Engineering ATTN: R. T. Davis M. J. Werle Cincinnati, OH 45221
1	University of Colorado Dept of Astro-Geophysics ATTN: E. R. Benton Boulder, CO 80302
2	University of Maryland ATTN: W. Melnik J. D. Anderson College Park, MD 20740
2	University of Michigan Dept of Aerospace Engineering ATTN: Technical Library M. Sichel East Engineering Building Ann Arbor, MI 48102
1	University of Washington Dept of Mechanical Engineering ATTN: Technical Library Seattle, WA 98195
1	Virginia Polytechnic Institute Dept of Aerospace Engineering ATTN: G. R. Inger Blacksburg, VA 24061

Aberdeen Proving Ground

Marine Corps Ln Ofc
Dir, USAMSAA
Dir/Cdr, USA CSL, EA
ATTN: Munitions Sys Division
E. A. Jeffers
W. C. Dee
W. J. Pribyl
(Bldg 3330)
Armament Concepts Ofc
DRDAR-ACW, M.C. Miller
(Bldg 3516)